On the Possibility That Cyclodextrins' Chiral Cavities Can Be Available on AOT *n*-Heptane Reverse Micelles. A UV−Visible and Induced Circular Dichroism Study

O. Fernando Silva,[†] Juana J. Silber,[‡] Rita H. de Rossi,[†] N. Mariano Correa,*[,‡] and Mariana A. Fernández*[,†]

Instituto de Investigaciones en Físico-Química de Córdoba (INFIQC), Facultad de Ciencias Químicas, Departamento de Química Orgánica, Universidad Nacional de Córdoba, Ciudad Universitaria, (X5000HUA) Córdoba, Argentina, and Departamento de Química, Universidad Nacional de Río Cuarto, Agencia Postal # 3, (X5804ALH) Río Cuarto, Argentina

Received: March 28, 2007; In Final Form: June 22, 2007

The formation of reverse micelles (RMs) of sodium 1,4-bis(2-ethylhexyl)sulfosuccinate (AOT) in *n*-heptane including two different β-cyclodextrin (β-CD) derivatives (hydroxypropyl-β-CD, hp-β-CD, and decenyl succinyl-β-CD, Mod-β-CD) is reported. Both cyclodextrins can be incorporated into AOT RMs in different zones within the aggregate, while β-CD cannot. Using UV−vis and induced circular dichroism (ICD) spectroscopy and different achiral molecular probes (some azo dyes, *p*-nitroaniline and ferrocene), it was possible to determine that Mod-β-CD is located with its cavity at the oil side of the AOT RM interface, while for hp-β-CD the cavity is inside the RM water pool. Among the molecular probes used, methyl orange (MO) was the only one which gave the ICD signal when dissolved in the AOT RMs with hp-β-CD, so a detailed study of MO behavior in homogeneous media was also performed to compare with the microheterogeneous media. The solvatochromic behavior of the dye depends not only on the polarity of the media but also on other specific solvent properties. A Kamlet−Taft analysis shows that the MO absorption spectrum shifts to longer wavelength with an increase in the solvent polarity−polarizability (π^*) and the hydrogen donor ability (α) of the medium. MO appears to be almost 3 times more sensitive to the π^* parameter than to the α parameter. In addition, from the MO absorption spectral changes with the hp-β-CD concentration, the association equilibrium constants in pure water (K_{11W}) and inside the RMs (K_{11RM}) were computed. The results show that K_{11W} is almost 10 times larger than the value inside the RMs. The latter can be explained considering that MO resides anchored to the RM interface through hydrogen bond interaction with the hydration bound water. This study shows for the first time that the cyclodextrin chiral cavity is available for a guest in an organic medium such as the RMs; therefore, we have created a potentially powerful nanoreactor with two different confined regions in the same aggregate: the polar core of the RMs and the chiral hydrophobic cavity of cyclodextrin.

Introduction

Several surfactants are able to aggregate in nonaqueous solvents to yield reverse micelles (RMs). Small solute particles can be located in three different compartments: (a) the external organic solvent, (b) the micellar interface formed by a surfactant monolayer, and (c) the internal water pool. Subsequently, these systems contain aqueous microdroplets entrapped in a film of surfactant and dispersed in a low-polarity bulk solvent.[1−11]

Among the anionic surfactants that form RMs, the best known are the systems derived from the sodium 1,4-bis(2-ethylhexyl)-sulfosuccinate (AOT) in different nonpolar media. AOT has a well-known V-shaped molecular geometry, giving rise to stable RMs without cosurfactant. In addition, it has the remarkable ability to solubilize a large amount of water with values of W ($W = [H_2O]/[AOT]$) as large as 40−60 depending on the surrounding nonpolar medium, the solute, and the temperature. However, the droplet size depends only on W.[2,3,5]

Cyclodextrins (CDs) are a group of well-known cyclic oligosaccharides that are capable of forming reversible noncovalent complexes with a wide variety of guests.[12] These macrocycles consist of several α-D-glucopyranose residues (six, seven, or eight rings, named α-, β-, and γ-CD, respectively) linked by α-1,4 glycosidic bonds. They have a doughnut-shaped structure in which the cavity has a hydrophobic character but the rims, in which the primary and secondary OH groups are inserted, are hydrophilic.

It is well-documented[13−15] that cyclodextrins form inclusion complexes with a variety of inorganic and organic molecules in solution. The formation of host−guest complexes occurs through desolvation of both species. Nevertheless, the stability of the complex is related to the amount of water that can be released by the cyclodextrin upon encapsulation of the guest molecule.[16,17] Connors[18] reported that amphiphilic compounds such as surfactants form highly stable complexes. As a consequence of the binding process, some properties of the target molecule can be dramatically changed. This is the case for amphiphiles that form micelles or any other type of aggregate. In this situation, the presence of CDs introduces a new equilibrium into the medium, and this competes with the self-

* Authors to whom correspondence should be addressed. E-mail: mcorrea@exa.unrc.edu.ar (N.M.C.); marfer@fcq.unc.edu.ar (M.A.F.).
[†] Universidad Nacional de Córdoba.
[‡] Universidad Nacional de Río Cuarto.

10.1021/jp0724424 CCC: $37.00
Published on Web 08/17/2007

assembly process, normally causing the destruction of the aggregates.[19−21]

Recently, it was demonstrated that in systems containing nonionic surfactants of increasing hydrophobicity the percentage of uncomplexed CD increases with the hydrophobic character of the surfactant.[22] This result is a consequence of the dynamic behavior shown by the mixed CD−surfactant systems, where the concentration of uncomplexed CD is the result of the balance between the complexation processes of the surfactant with the CD and the auto-aggregation (micellization) processes of the surfactant. The results demonstrate that, on decreasing the surfactant critical micelle concentration (cmc), the percentages of uncomplexed CD can increase to almost 95%.[20]

With the aim of optimizing the properties of cyclodextrins for a particular use, many substituted CDs have been prepared and new derivatives continue to be reported.[23] It has been shown that macrocyclic amphiphiles of hydrophobically modified CDs can form a variety of supramolecular assemblies, including monolayers, multilayers, and Langmuir−Blodgett films at the air−water interface.[24] Moreover, amphiphilic CDs can be admixed to phospholipid monolayers[25] as well as liposomes, and they can be dispersed into nanospheres, thus showing promising properties for drug encapsulation.[26]

It is known that a unique microenvironment for carrying out a variety of chemical and biochemical reactions is found in the polar cores of RMs and the chiral hydrophobic cavity of CDs. RMs have been used as model systems for studying various reactions in confinement, for example, biological functions, such as enzymatic reactions[27−30] or micellar catalysis.[31−36] Despite their simplicity, they provide an excellent method to study the fundamental effects of confinement.

Due to the unique catalytic properties of RMs and to the chiral properties of the CD cavity, in this contribution, we characterized RMs made with AOT and two different cyclodextrins solubilized in different zones within the aggregate: hydroxypropyl-β-CD (hp-β-CD) and decenyl succinyl-β-CD (Mod-β-CD) (Scheme 1). The idea is to try to create a novel medium with different confined regions in the same aggregate: the polar core of the RMs and the chiral hydrophobic cavity of the cyclodextrins that may be used as a chiral nanoreactor.

In this work, we report that Mod-β-CD and hp-β-CD can be incorporated into AOT RMs while β-CD cannot. Moreover, our study shows for the first time that the cyclodextrin chiral cavity may be available for a guest in an organic medium such as the RMs.

Experimental Section

Sodium 1,4-bis(2-ethylhexyl)sulfosuccinate (AOT) (Sigma >99% purity) was used as received and was kept under vacuum over P_2O_5 to minimize H_2O absorption. The absence of acidic impurities was confirmed through the 1-methyl-8-oxyquinolinium betaine (QB) absorption bands.[37]

n-Heptane and benzene (Merck, HPLC quality) were used as received.

The molecular probes *p*-nitroaniline (Carlo Erba) and ferrocene (Sigma) were used as received. The azo compounds were samples existent in the laboratory from previous work.[38,39]

β-Cyclodextrin[40] and hp-β-CD (Aldrich, average degree of substitution = 5.7 per cyclodextrin molecule) were used as received, but the purity was periodically checked by UV spectroscopy. Mod-β-CD (average degree of substitution = 1 per cyclodextrin molecule) was synthesized in the laboratory following the procedure in the literature[41] by the reaction of 2-decen-1-ylsuccinic anhydride and β-CD.

SCHEME 1: Structures of the Different Cyclodextrins Used in This Work

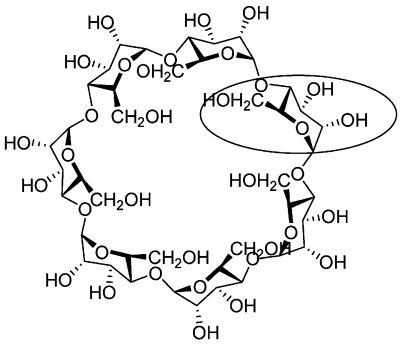

β-CD

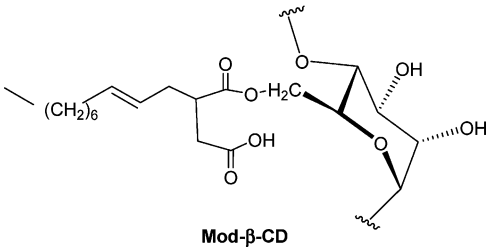

Mod-β-CD

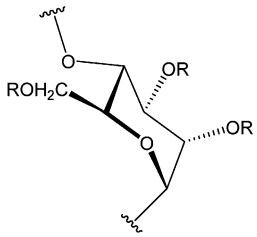

R=one or more -$CH_2CH(OH)CH_3$ moieties

hp-β-CD

For the determination of the association constants of methyl orange (MO)−hp-β-CD complexes, absorption spectra of solutions containing a constant organic guest concentration and increasing concentrations of hp-β-CD were recorded on a spectrophotometer. The procedure was as follows: a stock solution of the dye in water or RM medium was prepared. The cyclodextrin was dissolved with an aliquot of this solution. Then, the solutions to be measured were prepared by combination of the adequate volumes of the two stock solutions, with and without the host.

The solutions of the probes with Mod-β-CD were prepared in buffer with a pH of 10.6 (HCO_3^-/CO_3^{2-}) due to the low solubility of the host in water.

To perform the study in pure solvents, an appropriate amount of MO stock solution in acetonitrile (Sintorgan HPLC grade) was transferred into the volumetric flask using a calibrated microsyringe. The solvent was evaporated by bubbling dry N_2, and the residue dissolved in the appropriate solvent (HPLC grade) to obtain a final MO concentration of around 10^{-5} M. Ultrapure water was obtained from Labonco equipment model 90901-01.

The absorption spectra were measured by using Shimadzu 2101 PC or Shimadzu MultiSpec 1501 spectrometers at 25.0 ± 0.1 °C. The induced circular dichroism spectra were measured using a JASCO J-810 instrument. The path length used in all spectroscopic experiments was 1 cm.

To apply the Kamlet−Taft solvatochromic comparison method (KTSCM), the solvent set was chosen to cover a range as wide

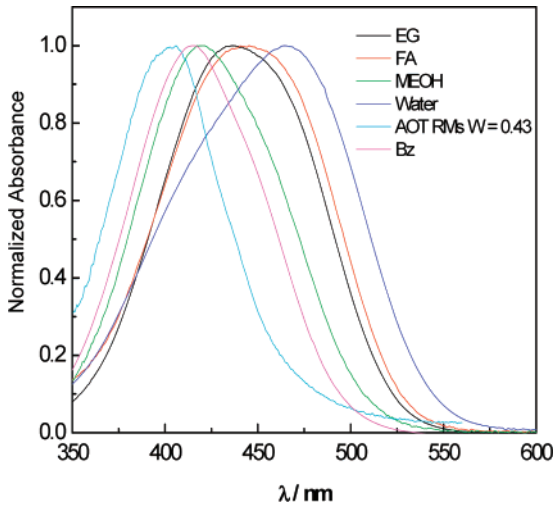

Figure 1. Normalized absorption spectra of MO in homogeneous media and in AOT RMs at [AOT] = 0.30 M and $W = 0.43$. EG, ethylene glycol; FA, formamide; MEOH, methanol; Bz, benzene.

as possible in the various solvent characteristics which also show significant variation in the spectroscopic properties.

The stock solutions of AOT in *n*-heptane solvent were prepared by mass and volumetric dilution. To obtain optically clear solutions, they were shaken in a sonicating bath. To introduce the probes, concentrated solutions of the molecular probes were prepared in acetonitrile (Sintorgan HPLC quality). The appropriate amount of these solutions to obtain the desired final concentration of molecular probe in the micellar system, $\sim 10^{-5}$ M, was transferred into a volumetric flask, and the acetonitrile was removed by bubbling dry N_2. *n*-Heptane was added to the residue, and the resulting solution was used to prepare the surfactant containing samples. The appropriate amount of stock surfactant solution to obtain a 0.3 M concentration of surfactant in the micellar media was transferred into the cell, and the water was added using a calibrated microsyringe.

The diameters of the RMs were determined by dynamic light scattering (DLS, Malvern 4700 with goniometer and 7132 correlator) with an argon-ion laser operating at 488 nm. All measurements were made at a scattering angle of 90° at a temperature of 25 °C.

Results and Discussion

Methyl Orange's Solvatochromism. Previous solvatochromic studies performed on the electronic transition energy of the probe, methyl orange (MO), show that the molecule exhibits an extreme sensitivity of the absorption wavelength to the polarity of the probe's environment.[42−46] Nevertheless, there are certain facts that are still unclear in regard to the electronic transitions responsible for the observed effects. Figure 1 shows MO's electronic absorption band in different solvents, and it can be seen that the band is unsymmetrical in every solvent studied regardless of their properties. Moreover, in water, the band has a hump at the high-frequency side of the absorption maximum, while, in the other solvents, the hump is on the low-frequency side. It is known[47,48] that in organic solvents the electronic spectra of azo dyes like MO have a superposition of a $\pi-\pi^*$ and $n-\pi^*$ transitions. It has been proposed that, as the polarity of the medium increases, the $\pi-\pi^*$ transition shifts to the visible region and the $n-\pi^*$ transition acquires additional intensity because of the sustituents' perturbations.[48]

On the other hand, the feature of the MO electronic band in water is quite interesting and different explanations have been proposed to attempt an interpretation. Some authors claim that the absorption band for MO in water consists of two overlapping transitions with equal intensity of $n-\pi^*$ and charge transfer character.[48] Alternatively, other authors[49−51] believe that the visible spectra of MO can be explained by the combination of two bands centered at around $\lambda = 476$ nm and $\lambda = 417$ nm which are due to a single electronic transition that corresponds to different species in equilibrium in solution: (i) a hydrogen bonded complexed azo species ($\lambda = 476$ nm) and (ii) a free azo species ($\lambda = 417$ nm). In water, the contribution of the low-energy band is very important, whereas the high-energy band predominates in organic solvents. The low-energy band is attributed to the $\pi-\pi^*$ transition which is red-shifted due to hydrogen bonded interactions between water and the azo nitrogens, whose basicity is enhanced by the *p*-amino group of MO.[49,51,52] There are other possibilities that might be taken into account to explain the shape of the MO absorption band in water. For example, MO can aggregate spontaneously in aqueous solution, but this possibility is discounted because the dye obeys Beer's law in the whole concentration range employed in this work (concentration 4.87×10^{-7} to 1.22×10^{-4} M). Besides, deconvolution of the spectrum in two bands centered at 467 and 400 nm leads to a set of spectra where the ratio of the absorption maxima is independent of the concentration (results not shown). The same was found previously by other authors.[46,53] Another possibility could be the existence of trans−cis isomers. This is very unlikely because the more stable isomer of the azo compounds is the trans isomer and, at room temperature, the conversion of cis into trans is a very fast process.[38,39,54] Moreover, several authors have ruled out this possibility.[49,52]

TABLE 1: Wavenumbers (ν_{abs}) of the Maxima of Absorption for MO in Different Solvents

N⁰	solvents	λ/nm	$\nu_{abs}/10^{-3}$ cm^{-1}	π^{*d}	α^d
1	*n*-heptane[a,b]	396	25.25	−0.08	0.00
2	cyclohexane[a,b]	394	25.38	0.00	0.00
3	*n*-hexanol[a]	417	23.98	0.40	0.80
4	*n*-octanol[a]	416	24.04	0.40	0.77
5	*n*-pentanol[a]	417	23.98	0.40	0.84
6	*t*-butanol	412	24.30	0.41	0.42
7	*n*-decanol[a]	416	24.04	0.45	0.70
8	*n*-butanol[a]	417	23.98	0.47	0.84
9	*n*-propanol[a]	417	23.98	0.52	0.84
10	ethanol	417	23.98	0.54	0.89
11	benzene	406	24.63	0.55	0.00
12	dioxane[b,c]	412	24.27	0.55	0.00
13	methanol	420	23.81	0.60	0.91
14	acetone	412	24.27	0.62	0.00
15	acetonitrile[a,b]	416	24.01	0.66	0.19
16	chlorobenzene[a,b]	411	24.33	0.71	0.00
17	dimethyl formamide[a,b]	421	23.74	0.88	0.00
18	ethylene glycol	442	23.02	0.92	0.90
19	formamide	447	22.37	0.97	0.71
20	dimethyl sulfoxide[c]	429	23.31	1.00	0.00
21	water	467	21.41	1.09	1.17

[a] Values taken from ref 44. [b] Values taken from ref 46. [c] Values taken from ref 42. [d] Values taken from refs 56−58.

Table 1 shows the absorption maxima of MO in a series of selected solvents. In light of our results presented in Figure 1 and in Table 1, we believe that a composite of the explanations shown above is adequate to explain the MO absorption band in the different media studied. Looking at the shape of the spectrum for MO in different solvents, we can see that the absorption bands have a shoulder in the low-energy side of MO's band not only in all of the monohydroxi substituted solvents but also in solvents that are not hydrogen bond donors such as benzene and acetone (not shown). Moreover, in all of these solvents,

the high-energy band, which should correspond to non-hydrogen-bonded species, is predominant. It seems to us that a superposition of two $\pi-\pi^*$ transitions seems to be responsible for the shape of the MO absorption band in these media.[51,52,55]

Figure 1 also shows that in solvents that have high polarity−polarizability (π^*) and hydrogen bond donor ability (α), such as formamide, ethyleneglycol, and water, a new low-energy band emerges. This band is assigned to a $\pi-\pi^*$ transition that is red-shifted due to hydrogen bond interactions with these solvents.[49,51] In other words, in solvents that are both strong polar and strong hydrogen bond donor media, there is an equilibrium between solvation species, each one having a unique electronic transition.

To gain more insight into the MO sensitivity to different environments, its electronic absorption spectra were analyzed considering the set of solvents with different properties. The solvent effects on physical or chemical processes are usually studied by means of empirical solvent parameters to determine which type of interactions predominates. One of the most useful approaches elucidating and quantifying different solute−solvent interactions is the Kamlet−Taft solvatochromic comparison method (KTSCM).[56] According to this, the absorption and emission band wavenumbers (ν) can be correlated using eq 1:

$$\nu = \nu_o + s\pi^* + a\alpha + b\beta \quad (1)$$

where π^* is the polarity−polarizability parameter, α is related to the hydrogen bond donation ability of the solvent, and β is a measure of the hydrogen bond acceptance or electron pair donation ability to form a coordinated bond. The *s*, *a*, and *b* coefficients measure the relative sensitivity of ν to the indicated solvent property.[57] The absorption maxima and the solvent parameters π^* and α[57,58] are given in Table 1.

The wavenumbers of the maxima of the MO absorption spectra (ν_{abs}) were used to obtain the KTSCM coefficients *s* and *a* which are given in eq 2. The confidence level of the regression is 99.5% according to a *t*-test. In the correlation shown in eq 2, where n = number of solvents used and r = regression coefficient, the β parameter was not statistically significant and it was not included. It must be pointed that solvents 18, 19, and 21 strongly deviate from the correlation. The reason may be that in these solvents there is equilibrium between different hydrogen bonded complexes (see above).

$$\nu_{abs} = (25.28 \pm 0.09) - (1.69 \pm 0.14)\pi^* - (0.63 \pm 0.10)\alpha \quad (2)$$

$$n = 18,\ r = 0.960$$

The result shows that MO displays a bathochromic shift with π^* and α. The sensitivity of MO to the α parameter is expected, as it can accept a hydrogen bond through its azo, amino, and SO_3^- groups. The *s*/*a* ratio is ~2.68, demonstrating that MO is almost 3 times more sensitive to the polarity parameter (π^*) than to the hydrogen bond donor ability of the solvent (α). This is reasonable considering that the molecule is very polarizable due to extended resonance. The higher sensitivity to π^* compared to α may also explain why, in the MO absorption spectra, the band of hydrogen bonded complexes is seen only in solvents with high values of α.

Complexation of Methyl Orange with Cyclodextrins in Water. Among all of the molecular probes studied in this work (see Scheme 2), MO was the only one that showed complexation with hp-β-CD in RMs, so this complexation was first studied in water before extending the investigation to RM media.

SCHEME 2: Structures of the Molecular Probes and the Surfactant Used in This Work

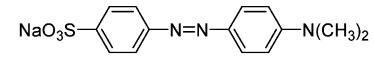

Methyl orange (**MO**)

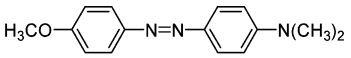

4-dimethylamino-4′-methoxyazobenzene (**AZ**)

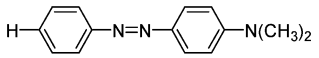

Methyl yellow (**MY**)

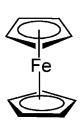

ferrocene

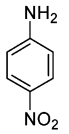

p-nitroaniline (**p-NA**)

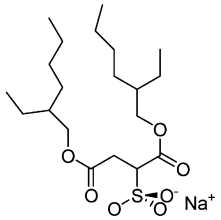

AOT

Figure 2A shows the absorption spectra of MO in water at different concentrations of hp-β-CD. A small blue shift of the visible absorption band is observed as the concentration of hp-β-CD is increased, leading to the absorbance concentration profile shown in Figure 2B. According to our results in homogeneous media, a hypsochromic shift of the MO absorption band can be attributed to a decrease in the polarity and the hydrogen bond donor abilities of the environment. Indeed, we attributed the feature shown in Figure 2 to the interaction between MO and hp-β-CD to form an inclusion complex. Most of the variations observed could be explained by the formation of a 1:1 complex, and the system can be described as in eq 3,[59,60] where MO...hp-β-CD stands for the hp-β-CD−MO complex and K_{11W} is the equilibrium constant for the association in water.

$$\text{MO} + \text{hp-}\beta\text{-CD} \overset{K_{11W}}{\rightleftharpoons} \text{MO...hp-}\beta\text{-CD} \quad (3)$$

At any wavelength, the observed absorbance is the sum of the absorbances of each contributing species, which are proportional to their equilibrium concentrations. These concentrations can be obtained using the mass balances for MO and hp-β-CD and the definition of the association equilibrium constant (K_{11W}). Following this procedure and under conditions of excess hp-β-CD concentration (where [hp-β-CD] ≅ [hp-β-CD]$_0$), the change in absorbance compared to the value in pure water (ΔA) at constant wavelength is given by eq 4:[51,59]

$$\Delta A = \frac{\Delta\epsilon_{11W} K_{11W} [\text{hp-}\beta\text{-CD}]_0 [\text{MO}]_0}{1 + K_{11W}[\text{hp-}\beta\text{-CD}]_0} \quad (4)$$

where [hp-β-CD]$_0$ and [MO]$_0$ represent the initial concentration of the hp-β-CD and that of the MO, respectively; $\Delta\epsilon_{11W}$ is the difference in the molar absorptivity between the free and

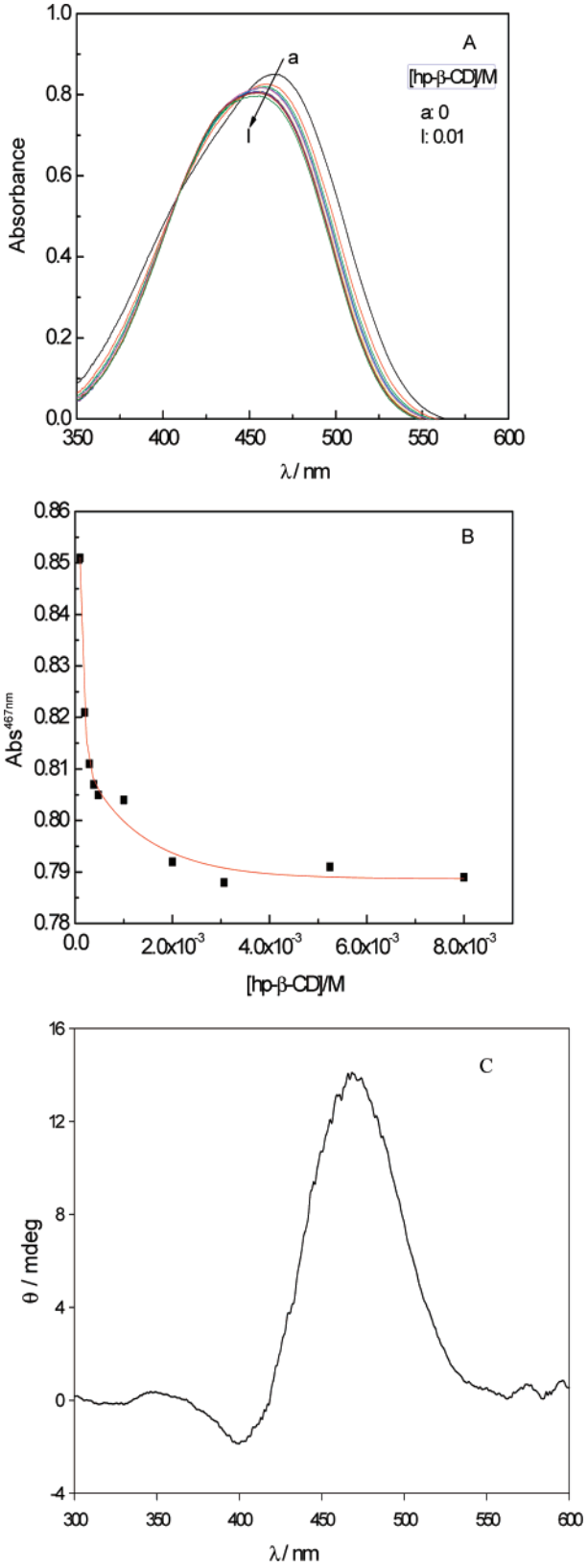

Figure 2. (A) Absorption spectra of MO in water in the presence of different concentrations of hp-β-CD, varying from 0 to 0.01 M, [MO] $= 1.8 \times 10^{-5}$ M. (B) Variation of absorbances at 467 nm as a function of hp-β-CD concentration. The red line represents the fitted curve by eq 4. (C) ICD spectrum of the hp-β-CD−MO complex in water, [hp-β-CD] $= 5 \times 10^{-3}$ M, [MO] $= 5 \times 10^{-5}$ M.

complexed substrate. The absorbance at $\lambda = 467$ nm was fitted to eq 4 using a nonlinear least-squares program,[61] and the value of K_{11W} was calculated as $(7.6 \pm 0.9) \times 10^3$ M^{-1}. Measurements at other wavelengths gave the same value within experimental error. In a recent work,[51] the formation of inclusion complexes between MO and β-CD was studied using UV−visible absorption spectroscopy. The authors have found two complexes of stoichiometries 1:1 and 1:2, as determined by principal components analysis of the absorption data. This method yields precise values of the corresponding association constants which gives the following values: $K_{11} = 2.97 \times 10^3$ M^{-1} and $K_{12} = 0.1 \times 10^3$ M^{-1}. They have concluded that the equilibrium concentration of the 2β-CD−MO complexes is only important when β-CD is in large excess, since K_{12} is much smaller than K_{11}. In this way, for the concentration range of cyclodextrins used, our assumption of the 1:1 complex formation seems correct. The value of K_{11W} calculated here for the interaction of MO with hp-β-CD is very close to that reported for the 1:1 interaction of MO with β-CD.[51] The similarity of association constants of compounds with hp-β-CD and β-CD is very common.[62,63]

Since cyclodextrin is a chiral molecule, an induced circular dichroism (ICD) signal is expected when an achiral guest molecule, such as MO, is included in its cavity.[64−66] Thus, we have investigated the ICD spectra of the hp-β-CD−MO complexes in aqueous solution. Figure 2C shows these results. The development of an ICD signal will be used as a tool to determine the location of the cyclodextrins inside RM solutions (see below).

Cyclodextrins in AOT Reverse Micellar Media. We have investigated the solubilization of different cyclodextrins: β-CD, Mod-β-CD, and hp-β-CD in AOT RMs at different W values. Also, for comparison we have tested α- and γ-CDs which are more soluble in water.[67] It turns out that α-, β-, and γ-CD cannot be solubilized in the RM system at any W value. It seems that the hydrogen bond interaction between the CD hydroxyl group and the AOT polar headgroup, although a very effective H-bond acceptor,[5,68−71] is not strong enough to solubilize these cyclodextrins. It is known that OH groups of cyclodextrins and in particular β-CD form very strong intramolecular hydrogen bonds,[72] and it may be possible that the polar headgroup of AOT cannot compete with these intramolecular interactions.

On the other hand, hp-β-CD which has their OH groups substituted by the hydroxypropyl group has weaker intramolecular hydrogen bonds and thus a greater tendency to interact with the environment. Proof of this is the fact that the solubility in water at room temperature of β-CD is 0.0185 g/mL[67] while that of hp-β-CD is 0.55 g/mL.[73]

Mod-β-CD (see Scheme 1), due to the presence of the long hydrocarbon tail in its moiety, resembles a surfactant molecule which is capable of self-aggregating in water with a cmc of 1.7×10^{-4} M. Mod-β-CD can be solubilized in the AOT RMs at $W > 20$ and up to [Mod-β-CD] $= 1 \times 10^{-3}$ M. It is clear that the presence of the hydrocarbon tail helps the solubilization of this cyclodextrin, since the β-CD is not solubilized under the same conditions. In other words, it seems to act as cosurfactant and the molecule resides at the RM interface. Since addition of hp-β-CD or Mod-β-CD to the microemulsion could change the characteristics of the solution,[74] we performed dynamic light scattering experiments to compare the size of RMs containing water and cyclodextrin solutions. The sizes of the RMs can be measured with an overall AOT concentration of 0.3 M because the viscosity of the solution is the same as that in *n*-heptane. Dynamic light scattering experiments showed that, for RMs with $W = 30$ formed without and with cyclodextrins, the hydrodynamic radius (6.1 nm) and polydispersity are the same. This indicates that solubilization of any of the cyclodextrins in the

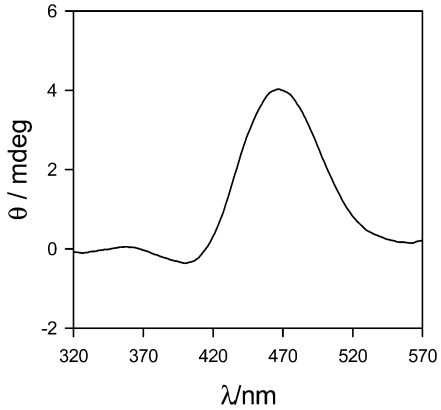

Figure 3. Induced circular dichroism spectra of the hp-β-CD−MO complex in AOT RMs. [AOT] = 0.3 M; W = 30; [hp-β-CD] = 5×10^{-3} M; [MO] = 2.6×10^{-5} M.

RMs changes neither their size nor their shape and RMs are not perturbed by dissolution of these molecules.

According to the hp-β-CD and Mod-β-CD structures (Scheme 1), it is clear that they have to be located in different zones within the RM media. In order to obtain an idea of these locations, we have performed ICD experiments using several molecular probes. The molecules were chosen with different structures (see Scheme 2) to allow them to reside in different zones within the aggregates. The azo dyes are polarity probes that are known to interact with β-CD;[59] therefore, they could provide information about the location of the CD cavity in the RMs. Ferrocene is a very water insoluble compound that has a large association constant with β-CD;[75] consequently, it may interact with the CD if both molecules are located close enough in the RMs. Finally, *p*-NA is a probe that was extensively studied in RMs,[5,68] so its location in the microheterogeneous system free of cyclodextrin is well-known. The combination of the experimental results obtained with the different probes could provide information about the position of the chiral cavity of the cyclodextrin in the microheterogeneous system.

On the basis of the molecular probe structure, it can be predicted that *p*-NA and MO would be located in the polar core of the RMs. This expectation is based on the strong H-bond donor ability for *p*-NA[5,68] and the negative charge and insolubility in the *n*-heptane pseudophase in the case of MO.[42,43] On the other hand, the nonionic azo dyes AZ and MY (Scheme 2) and ferrocene would partition between the organic and the AOT RM pseudophases.[5] Besides, since all of them are achiral guest molecules, they do not give an ICD signal in the AOT RMs without cyclodextrins.

p-NA and MO, which are water soluble probes, give comparable ICD signals with both cyclodextrins in pure water. This result shows that they are included in the cavity of the chiral cyclodextrins in homogeneous media. AZ, MY, and ferrocene are insoluble in water, but it is known that they form inclusion complexes with the cyclodextrins in binary mixtures of ethanol and water.[59,76] However, the behavior of the probes is quite different when the cyclodextrins are encapsulated inside the RMs. The experimental conditions that we have used in the microheterogeneous media were identical to those used in homogeneous media, i.e., [molecular probe] $\cong 10^{-5}$ M and [cyclodextrins] $\cong 10^{-3}$ M. For Mod-β-CD, there were no ICD signals for any of the molecular probes tested positive in homogeneous media. For hp-β-CD inside the RMs only there is a clear ICD signal when MO is used. Figure 3 shows the ICD spectra of hp-β-CD−MO complexes in AOT RMs ([AOT] = 0.3 M, W = 30, [hp-β-CD] = 5×10^{-3} M, [MO] = 2.6×10^{-5} M). The fact that Mod-β-CD does not give the ICD signal inside the RMs with any of the molecular probes may indicate that the CD chiral cavity is located among the tails of the AOT surfactants and/or *n*-heptane molecules at the oil side of the RM interface and it is not available for the molecular probes studied. In a recent work, it was found that γ-CD functionalized at the 6-position with perfluoro butanoate groups could form a complex with AOT and could solubilize this surfactant in CO_2.[77] Also, it was found that β-CD in the presence of nonionic surfactants in water can form complexes with the surfactant monomers which compete with the aggregation process of the surfactant.[22] Indeed, it is likely that Mod-β-CD can complex with the AOT tails and/or *n*-heptane molecules at the AOT interface.

On the contrary, hp-β-CD interacts more strongly with water than Mod-β-CD;[78] therefore, it can be predicted that it will reside in the water pool within the AOT RMs. In this way, it shows the ICD signal with MO dye, which confirms that the cavity of the cyclodextrin is available for the guest even inside the RMs. This result is very challenging because, now, we have a chiral supramolecular structure (the cyclodextrin) inside an organized medium such as the AOT RMs, giving a novel medium to use as a nanoreactor. We think that *p*-NA is not included by the hp-β-CD cavity because the strong interaction with the AOT polar headgroup[5,68] does not allow the probe to be pulled toward the water pool where hp-β-CD exists in a measurable amount. It should be noted that the association equilibrium constant between β-CD and *p*-NA is 260 M^{-1},[79] and considering the results of MO (see below), we expect that the value in the RMs is about 10 times smaller. This gives an expected value for the association of about 26 M^{-1} which is difficult to measure under our experimental conditions.

The question of the location of the hp-β-CD and MO in AOT RMs remains. In order to obtain the ICD signal, different situations can be considered: (i) both hp-β-CD and MO reside in the water side of the interface, (ii) the molecules both reside in the water pool, (iii) hp-β-CD is in the water pool and MO is in the interface and the complex is formed in the water pool.

Often, intuition leads to the assumption that ionic probe molecules as well as very hydrophilic probes reside in the polar water pool of the RM systems.[5,80] Frequently, it is assumed that Coulomb repulsion from the anionic sulfonate headgroups of AOT should cause a negatively charged molecule, such as MO, to dive away from the interface toward the water pool.[5,81,82] A recent study challenged the assumption that ionic probe molecules reside solvated by the water in the microheterogenous environments and suggested that probe molecule location be carefully considered before interpreting data from RM media.[74,80] Indeed, following this advice, we have investigated the possible location of MO and hp-β-CD inside AOT RMs.

MO in AOT Reverse Micelle Media. Different experiments were performed to investigate the location of MO in AOT RMs. Thus, the concentration of AOT was varied in the range 0.01−0.15 M, at constant W in the AOT RM system without cyclodextrins. The MO absorption spectra (results not shown) show no variation with the surfactant concentration, which suggests that MO along with other molecular probes that are not soluble in the organic pseudophase resides exclusively inside the AOT RMs without partition to the organic solvent.[5,37,82,83] The situation is quite different when at a given AOT concentration W is varied. Figure 4A shows the absorption spectra of MO at [AOT] = 0.3 M as a function of W. The spectrum in water is also included for comparison. The results show that,

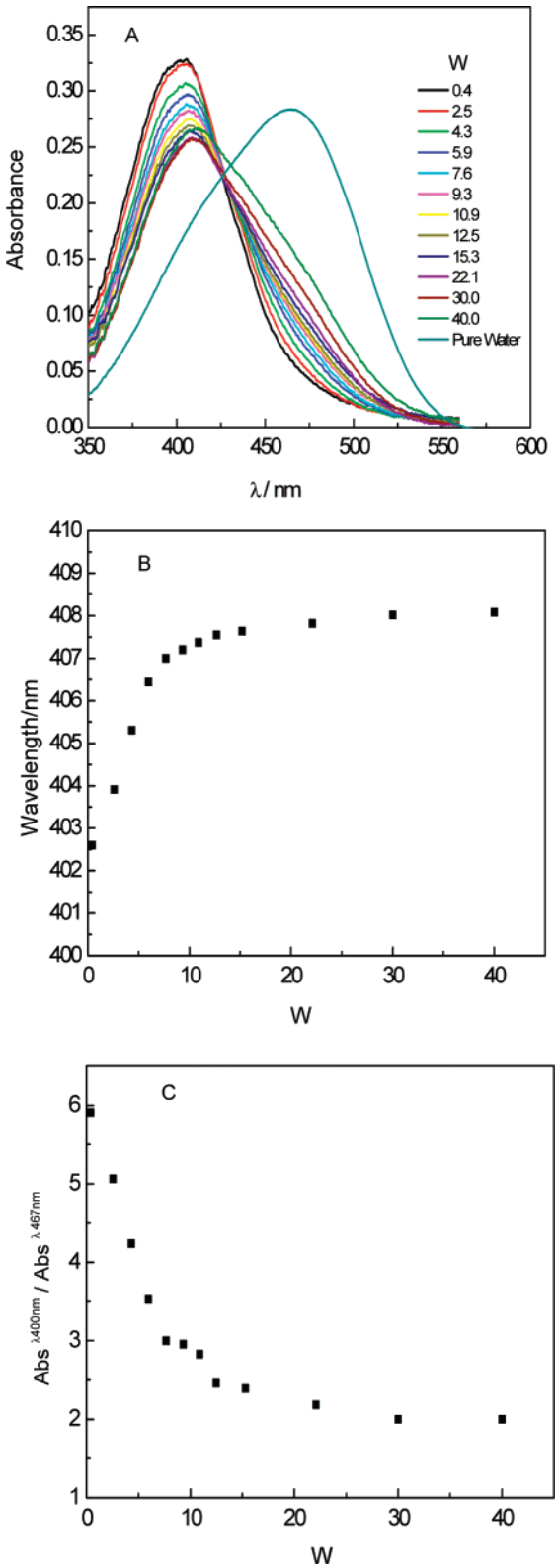

Figure 4. (A) Absorption spectra of MO in AOT RMs at different *W*s and in pure water. (B) Variation of MO absorption maxima with *W*. (C) Variation of $Abs^{\lambda 400nm}/Abs^{\lambda 467nm}$ as a function of *W*. [AOT] = 0.3 M, [MO] = 0.8×10^{-5} M.

upon the water addition, a new low-energy absorption band emerges and, even at $W = 40$, the spectrum is completely different from the one obtained in pure water. The plot of the wavelength maximum as a function of *W* (Figure 4B) reveals some interesting features. The band shifts to the red which reflects the increase in the micropolarity of the RM interface but never reaches the value of the maxima in pure water (467 nm). This red shift takes place up to $W = 10$, and then, the absorption maxima remains constant. The latter is a characteristic result for molecular probes that reside at the RM interface.[5,37] Consequently, sampling the RM interfacial region should lead the MO molecule to report on water with properties different from the bulk. At higher water content, $W > 10$, the interfacial properties in AOT RMs formed in aliphatic hydrocarbon solvents, such as *n*-heptane in the studies discussed here, become independent of water content. Similar results have been found in different AOT RMs under supercritical conditions[84−88] and in nonionic RMs with water[42,43,45] or encapsulated ionic liquid.[89,90] As these authors, we concluded that MO is most likely situated at the interface of the RMs, not positioned in the water pool despite the negative charge of the AOT and the molecular probe. It is also likely that the high ionic strength inside AOT RMs favors the MO ion pairing and thus decreases the effective charge of the MO molecules. As a consequence, MO has more of a tendency to reside at the AOT reverse micelle interface. A similar effect was reported for $[Fe(CN)_6]^{-4/3}$ inside AOT RMs.[91]

Figure 4A also shows the development of a new absorption band with a maximum around $\lambda = 467$ nm. The homogeneous media results have shown that when the solvents are very good as hydrogen bond donors, the red band can be attributed to hydrogen bond complexes between the solvent and the azo nitrogen. Figure 4C, which shows the ratio of $Abs^{\lambda 400nm}/Abs^{\lambda 467nm}$ as a function of *W*, reveals that the major changes occur up to $W = 10$ and, after that, the ratio remains constant. It seems to us that MO at the AOT RM interface interacts through hydrogen bonds with the hydration water up to $W = 10$, and then, it remains anchored at the interface due to this interaction. Similar results were found for a zwitterionic molecular probe, betaine 1-methyl-8-hydroxyquinolinium, in AOT RMs where, despite the high solubility of the probe in water, it remains at the interface because of the hydrogen bond interaction with the water molecules.[37,92]

Complexation of MO with hp-*β*-CD in AOT Reverse Micelles. The ability of MO to form inclusion complexes with hp-*β*-CD was further investigated inside AOT RMs to quantify the association equilibrium constant inside the RMs (K_{11RM}). As hp-*β*-CD and MO are both totally incorporated inside the RMs, eqs 3 and 4 can be used without any correction, as was previously discussed for the partition constant of substrates totally incorporated inside the aggregates.[5,27] Figure 5A shows the absorption spectra of MO in AOT RMs at [AOT] = 0.3 M and $W = 30$ at different concentrations of hp-*β*-CD. Several features should be noted in this spectral change: (i) A red shift of the visible absorption band from $\lambda = 411$ nm to $\lambda = 445$ nm is observed as the concentration of hp-*β*-CD increases. Also, there is a decrease in the MO absorbance band at $\lambda = 411$ nm. (ii) A well-defined isosbestic point is detected around 423 nm which indicates that only one type of complex is formed. This result is in contrast with the spectrum obtained in water solution where no isosbestic point is observed. In water (Figure 2A), the MO absorption band shifts hypsochromically with the hp-*β*-CD concentration and the changes were explained due to the complexation of MO with the nonpolar cavity of the cyclodextrin. The data shown in Figure 5A where a bathochromic shift is observed can only be explained if the inclusion of MO inside the cyclodextrin cavity occurs in a more polar environment in comparison with the AOT RM interface. We believe that hp-*β*-CD is in the water pool of the RMs and the inclusion complex process is formed in the water pool and not in the interface of

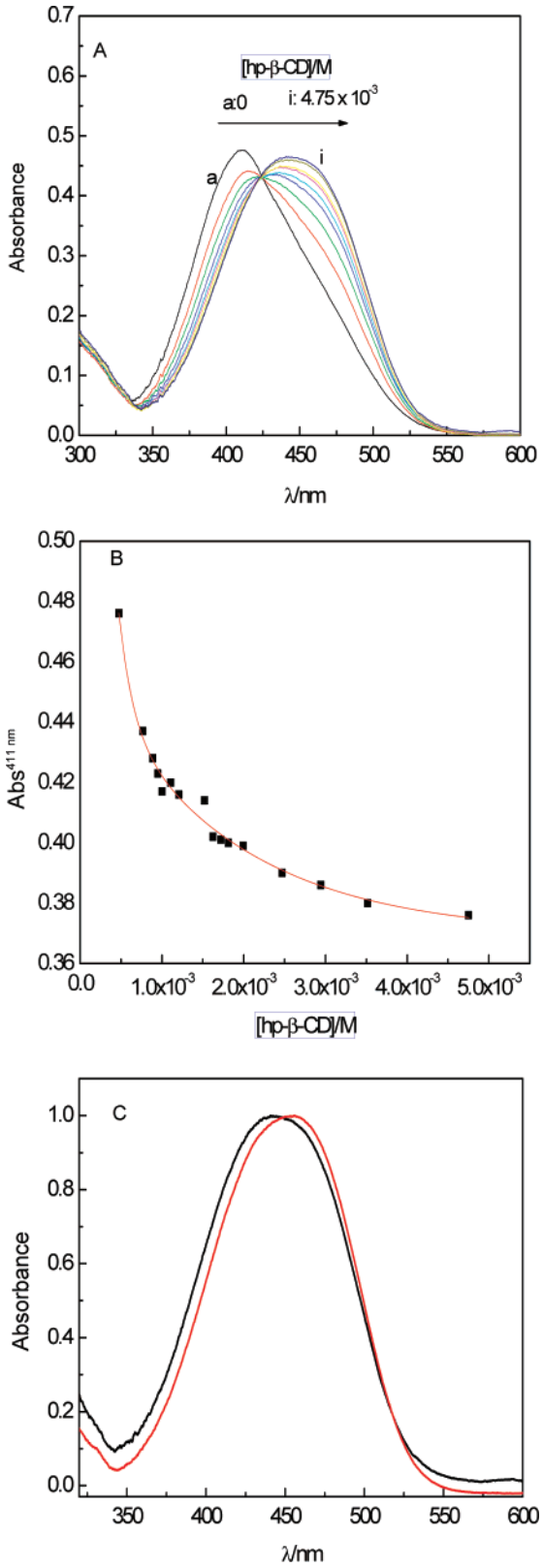

Figure 5. (A) Absorption spectra of MO in AOT RMs in the presence of different concentrations of hp-β-CD, varying from 0 to 4.75×10^{-3} M. [MO] = 1×10^{-5} M. (B) Variation of absorbances at 411 nm versus hp-β-CD concentration. The red line represents the fitted curve by eq 4. (C) Normalized absorption spectra of the hp-β-CD−MO complex in AOT RMs (black line) and in pure water (red line). [AOT] = 0.3 M; $W = 30$; [hp-β-CD] = 5×10^{-3} M; [MO] = 1×10^{-5} M.

the RMs, as is shown in eq 5, where MO_{int} stands for the MO molecules located at the RM interface.

$$MO_{int} + \text{hp-}\beta\text{-CD}_{\text{water pool}} \overset{K_{11RM}}{\rightleftharpoons} (\text{MO...hp-}\beta\text{-CD})_{\text{water pool}} \quad (5)$$

Figure 5B shows the absorbance changes with hp-β-CD concentration at $\lambda = 411$ nm, and Figure 5C shows the absorption spectra of the hp-β-CD−MO complex in water and in AOT RM media at [hp-β-CD] around 10^{-3} M in both cases. It is clear that the spectra of the complexes in both media are practically the same, in position and in shape, results that reinforce our interpretation that the inclusion process occurs in the water pool of the RMs. Indeed, though the MO spectrum at $W = 30$ is very different from the spectrum in pure water, the hp-β-CD−MO complex spectrum under the same conditions is practically the same as the one obtained in pure water. The least-squares fit of the data shown in Figure 5B to eq 4 allows us to calculate the values of $K_{11RM} = (7.5 \pm 0.7) \times 10^2$ M^{-1} for $W = 30$ and $K_{11RM} = (4 \pm 1) \times 10^2$ M^{-1} for $W = 15$ (spectra not shown). The measurements were done at two wavelengths, namely, 411 and 445 nm, and the values obtained were the same within experimental error. It is clear that K_{11RM} values are practically independent of the water content, results expected for a process that occurs in the water pool of the RMs. It must be pointed out that it was not possible to dissolve hp-β-CD at $W < 10$. On the other hand, the K_{11RM} value is around 10 times smaller than the K_{11W} value obtained in pure water: $K_{11W} = (7.6 \pm 0.9) \times 10^3$ M^{-1}. The results can be explained considering eqs 3 and 5. The main difference that can be seen between the complexation process in water and that in RMs is that, in the latter system, MO is anchored to the AOT RM interface through hydrogen bond interaction to the interfacial water. This interaction is so strong that, even at $W = 40$ and despite the negative charge of MO and its high water solubility, MO prefers to reside at the negative AOT RM interface rather than in the water pool. When hp-β-CD is added to the RMs, the situation is quite different. Now MO leaves the interface to make the inclusion complex with the cyclodextrin that is located in the water pool of the RMs. The driving force is strong enough to make the molecule leave the interface, but the equilibrium constant calculated under this condition is smaller than the one obtained in pure water presumably due to the strong interaction of MO with the hydration water at the interface. Another possibility could be that the inclusion complex forms at the AOT RM interface rather than in the water pool. Since the micropolarity at the AOT RM interfaces is always smaller than the value in the water pool,[5,37] the large red shift in the MO absorbance spectra shown in Figure 5A is not consistent with a process that occurs at the interface. The homogeneous studies show that the MO absorption band shifts bathochromically as the polarity and the hydrogen bond ability of the media increase. Thus, this red shift is probably due to the water pool environment where the inclusion complex formation occurs. Moreover, if the complexation process occurs at the interface, there will not be a match between the hp-β-CD−MO complex spectrum in water and that in the AOT RMs, as Figure 5C shows.

Conclusions

This study presents the investigation of novel AOT RMs made with the AOT surfactant, water, *n*-heptane, and two different cyclodextrins: hp-β-CD and Mod-β-CD. The results show, for the first time, that RMs with a chiral hydrophobic and hydrophilic nanostructured cavity in the same aggregates can be formed and that the cyclodextrin chiral cavity is available for a guest in an organic medium such as the RMs.

In AOT RMs, it was demonstrated that Mod-β-CD resides at the oil side of the RM interface with AOT tails and/or

n-heptane molecules inside its cavity. The situation is different for the more water soluble hp-β-CD which resides in the RM water pool and gives an ICD signal with MO. It is shown that MO resides at the AOT RM interface at every *W* value studied anchored through hydrogen bond interactions with the hydration water. When hp-β-CD is dissolved, the formation of the hp-β-CD−MO complexes in the water pool has to drive MO toward the water pool. Thus, the association equilibrium constant inside AOT RMs (K_{11RM}) is 10 times smaller than the value in pure water (K_{11W}).

The results allow exploration of the functionality of the interfaces, and it may be possible that these systems can be used as nanoreactors in asymmetric synthesis, a venue that we are currently investigating.

Acknowledgment. Financial support from the Consejo Nacional de Investigaciones Científicas y Técnicas (CONICET), Universidad Nacional de Río Cuarto, Universidad Nacional de Córdoba, Fundación Antorchas, and Agencia Nacional de Promoción Científica y Técnica is gratefully acknowledged. J.J.S., R.H.d.R., M.A.F., and N.M.C. hold a research position at CONICET. O.F.S. thanks CONICET for a research fellowship.

References and Notes

(1) Fendler, J. H. *Membrane Mimetic Chemistry*; Wiley: New York, 1982.
(2) Pileni, M. P. *Structure and Reactivity of Reverse Micelles*; Elsevier: New York, 1989.
(3) De, T. K.; Maitra, A. *Adv. Colloid Interface Sci.* **1995**, *59*, 95.
(4) Moulik, S. P.; Paul, B. K. *Adv. Colloid Interface Sci.* **1998**, *78*, 99.
(5) Silber, J. J.; Biasutti, M. A.; Abuin, E.; Lissi, E. *Adv. Colloid. Interface Sci.* **1999**, *82*, 189.
(6) Monduzzi, M.; Caboi, F.; Moriconi, C. *Colloids Surf., A* **1997**, *129−130*, 327.
(7) Hamada, K.; Ikeda, T.; Kawai, T.; Kon-No, K. *J. Colloid Interface Sci.* **2001**, *233*, 170.
(8) Kenéz, P. H.; Carlström, G.; Furó, I.; Halle, B. *J. Phys. Chem.* **1992**, *96*, 9524.
(9) Pileni, M. P. *J. Phys. Chem.* **1993**, *97*, 6961.
(10) Luisi, P. L.; Straub, B. *Reverse Micelles*, 8th ed.; Plenum Press: London, 1984.
(11) Ballesteros, A.; Bornscheuer, U.; Capewel, A.; Combes, D.; Condoret, J. S.; Koenig, K.; Kolisis, F. N.; Marty, A.; Mengue, U.; Scheper, T.; Stamatis, H.; Xenakism, A. *Biocatal. Biotransform.* **1995**, *13*, 1.
(12) D'Souza, V. T.; Lipkowitz, K. B. *Chem. Rev.* **1998**, *98*, 1741.
(13) Connors, K. A. *Chem. Rev.* **1997**, *97*, 1325.
(14) Raymo, F. M.; Stoddart, F. J. *Chem. Rev.* **1999**, *99*, 1643.
(15) Rekharsky, M. V.; Inoue, Y. *Chem. Rev.* **1998**, *98*, 1875.
(16) De Lisi, R.; Milioto, S.; Muratore, N. *Langmuir* **2000**, *16*, 4441.
(17) Inoue, Y.; Liu, Y.; Tong, L. H.; Shen, B. J.; Jin, D. S. *J. Am. Chem. Soc.* **1993**, *115*, 10637.
(18) Connors, K. A. *J. Pharm. Sci.* **1996**, *85*, 796.
(19) Gonzalez-Gaitano, G.; Sanz-Garcia, T.; Tardajos, G. *Langmuir* **1999**, *15*, 7963.
(20) Gonzalez-Gaitano, G.; Compostizo, A.; Sánchez-Martín, L.; Tardajos, G. *Langmuir* **1997**, *13*, 2235.
(21) Fernández, M. A.; de Rossi, R. H. *J. Org. Chem.* **2003**, *68*, 6887.
(22) Cabaleiro-Lago, C.; García-Río, L.; Hervés, P.; Mejuto, J. C.; Pérez Juste, J. *J. Phys. Chem. B* **2006**, *110*, 15831.
(23) (a) Motoyama, K.; Arima, H.; Hirayama, F.; Uekama, K. *J Inclusion Phenom. Macrocyclic Chem.* **2006**, *56*, 75. (b) Zhang, X. Y.; Sasaki, K.; Kuroda, Y. *J. Org. Chem.* **2006**, *71*, 4872. (c) Inoue, H.; Kawashita, T.; Nakayama, H.; Tsuhako, M. *Carbohydr. Res.* **2005**, *340*, 1766. (d) Delattre, F.; Woisel, P.; Bria, M.; Surpateanu, G. *Carbohydr. Res.* **2005**, *340*, 1706.
(24) (a) Kawabata, Y.; Matsumoto, M.; Tanaka, M.; Takahashi, H.; Irinatsu, Y.; Tamura, S.; Tagaki, W.; Nakahara, N.; Fukuda, K. *Chem. Lett.* **1986**, 1933. (b) Parrot-López, H.; Ling, C. C.; Zhang, P.; Baszkin, A.; Albrecht, G.; de Rango, C.; Coleman, A. W. *J. Am. Chem. Soc.* **1992**, *114*, 5479. (c) Tschoreloff, P. C.; Boissonnade, M. M.; Coleman, A. W.; Baszkin, A. *Langmuir* **1995**, *11*, 191. (d) Greenhall, M. H.; Lukes, P.; Kataky, R.; Agbor, N. E.; Badyal, J. P. S.; Yarwood, J.; Parker, D.; Petty, M. C. *Langmuir* **1995**, *11*, 3997. (e) Matsumoto, M.; Tanaka, M.; Azumi, R.; Tachibana, H.; Nakamura, T.; Kawabata, Y.; Miyasaka, T.; Tagaki, W.; Nakahara H.; Fukuda, K. *Thin Solid Films* **1992**, *210−211*, 803. (f) Nakahara, H.; Tanaka, H.; Fukuda, K.; Matsumoto, M.; Tagaki, W. *Thin Solid Films* **1996**, *284−285*, 687. (g) Parazak, D. P.; Khan, A. R.; D'Souza, V. T.; Stine, K. J. *Langmuir* **1996**, *12*, 4046. (h) Hamelin, B.; Jullien, L.; Laschewsky, A.; Hervé du Penhoat, C. *Chem.—Eur. J.* **1999**, *5*, 546.
(25) (a) Coleman, A. W.; Kasselouri, A. *Supramol. Chem.* **1993**, *1*, 155. (b) Kasselouri, A.; Coleman, A. W.; Baszkin, A. *J. Colloid Interface Sci.* **1996**, *180*, 384. (c) Kasselouri, A.; Coleman, A. W.; Albrecht, G.; Baszkin, A. *J. Colloid. Interface Sci.* **1996**, *180*, 398.
(26) (a) Jullien, L.; Lazrak, T.; Canceill, J.; Lacombe, L.; Lehn, J. M. *J. Chem. Soc., Perkin Trans.* **1993**, *2*, 1011. (b) Lin, J.; Creminon, C.; Perly, B.; Djedaïni-Pilard, F. *J. Chem. Soc., Perkin Trans. 2* **1998**, 2639. (c) Auzély-Velty, R.; Perly, B.; Taché, O.; Zemb, T.; Jéhan, P.; Guenot, P.; Dalbiez, J. P.; Djedaïni-Pilard, F. *Carbohydr. Res.* **1999**, *318*, 82. (d) Lesieur, S.; Charon, D.; Lesieur, P.; Ringard-Lefebvre, C.; Muguet, V.; Duchene, D.; Wouessidjewe, D. *Chem. Phys. Lipids* **2000**, *106*, 127.
(27) Falcone, R. D.; Biasutti, M. A.; Correa, N. M.; Silber, J. J.; Lissi, E.; Abuin, E. *Langmuir* **2004**, *20*, 5732.
(28) Martinek, K.; Levashov, A. V.; Klyachko, N. L.; Khmelnitski, Y. L.; Berezin, Y. V. *Eur. J. Biochem.* **1986**, *155*, 453.
(29) Durfor, C. N.; Bolin, R. J.; Sugasawara, R. J.; Massey, R. J.; Jacobs, J. W.; Schultz, P. G. *J. Am. Chem. Soc.* **1988**, *110*, 8713.
(30) Menger, F. M.; Yamada, K. *J. Am. Chem. Soc.* **1979**, *101*, 6731.
(31) Correa, N. M.; Durantini, E. N.; Silber, J. J. *J. Org. Chem.* **1999**, *64*, 5757.
(32) Correa, N. M.; Durantini, E. N.; Silber, J. J. *J. Org. Chem.* **2000**, *65*, 6427.
(33) Correa, N. M.; Zorzan, D. H.; Chiarini, M.; Cerichelli, G. *J. Org. Chem.* **2004**, *69*, 8224.
(34) Correa, N. M.; Zorzan, D. H.; D'Anteo, L.; Lasta, E.; Chiarini, M.; Cerichelli, G. *J. Org. Chem.* **2004**, *69*, 8231.
(35) Fernandes, M. L. M.; Krieger, N.; Baron, A. M.; Zamora, P. P.; Ramos, L. P.; Mitchell, D. A. *J. Mol. Catal. B: Enzym.* **2004**, *30*, 43.
(36) Khan M. N. *Micellar Catalysis*; Taylor & Francis: Boca Raton, FL, 2007.
(37) Correa, N, M.; Biasutti, M. A.; Silber, J. J. *J. Colloid Interface Sci.* **1995**, *172*, 71.
(38) Sánchez, A.; de Rossi, R. H. *J. Org. Chem.* **1993**, *58*, 2094.
(39) Sánchez, A.; de Rossi, R. H. *J. Org. Chem.* **1995**, *60*, 2974.
(40) Cyclodextrins were a gift from the pharmaceutical company Ferromet S. A., Buenos Aires, Argentina.
(41) González, C. J., de Rossi, R. H. *ARKIVOC* **2001**, *xii*, 87.
(42) Zhu, D-M.; Schelly, Z. A. *Langmuir* **1992**, *8*, 48.
(43) Zhu, D-M.; Schelly, Z. A. *J. Phys. Chem.* **1992**, *96*, 7121.
(44) Karukstis, K. K.; D'Angelo, N. D.; Loftus, C. T. *J. Phys. Chem. B* **1997**, *101*, 1968.
(45) Qi, L.; Ma, J. *J. Colloid Interface Sci.* **1998**, *197*, 36.
(46) Karukstis, K. K.; Savin, D. A.; Loftus, C.; D;Angelo, N. D. *J. Colloid Interface Sci.* **1998**, *203*, 157.
(47) Dyck, R. H.; McClure, D. S. *J. Chem. Phys.* **1962**, *36*, 2326.
(48) Rava, R. P. *J. Chem. Phys.* **1987**, *87*, 3758.
(49) Reeves, L. R.; Kaiser, R. S.; Maggio, M. S.; Sylvestre, E. A.; Lawton, W. H. *Can. J. Chem.* **1973**, *51*, 628.
(50) Lee, H.; Machida, K.; Kuwae, A.; Harada, I. *J. Raman Spectrosc.* **1983**, *14*, 126.
(51) Carrazana, J.; Reije, B.; Cabrer, P. R.; Al-Soufi, W.; Novo, M.; Vázquez Tato, J. *Supramol. Chem.* **2004**, *16*, 549.
(52) Brode, W. R.; Seldin, I. L.; Sporri, P. E.; Wyman, G. M. *J. Am. Chem. Soc.* **1955**, *77*, 2762.
(53) Buwalda, R. T.; Jonker, J. M.; Engberts, J. B. F. N. *Langmuir* **1999**, *15*, 1083.
(54) Sánchez, A. M.; Barra, M.; de Rossi, R. H. *J. Org. Chem.* **1999**, *64*, 1604.
(55) Oliveira, H. P.; Oliveira, E. G. L.; de Melo, C. P. *J. Colloid Interface Sci.* **2006**, *303*, 444.
(56) Kamlet, M. J.; Abboud, J. L. M.; Abraham, M. H; Taft, R. W. J. *J. Org. Chem.* **1983**, *48*, 2877.
(57) Abboud, J-L. M.; Notario, R. *Pure Appl. Chem.* **1999**, *71*, 645.
(58) Laurence, C.; Nicolet, P.; Dalati, M. T.; Abboud, J.-L. M.; Notario, R. *J. Phys. Chem.* **1994**, *98*, 5807.
(59) Sánchez, A. M.; de Rossi, R. H. *J. Org. Chem.* **1996**, *61*, 3446.
(60) Connors, K. A. *Binding Constants: the Measurement of Molecular Complex Stability*; John Wiley and Sons: New York, 1987.
(61) *SigmaPlot for Windows*, version 8.0; SPSS Inc., 2002.
(62) Takahashi, K. *Chem. Rev.* **1998**, *98*, 2013.
(63) Pacioni, N. L.; Veglia, A. V. *Anal. Chim. Acta* **2007**, *583*, 63.
(64) Shimizu, H.; Kaito, A.; Hatano, M. *Bull. Chem. Soc. Jpn.* **1979**, *52*, 2678.
(65) Shimizu, H.; Kaito, A.; Hatano, M. *Bull. Chem. Soc. Jpn.* **1981**, *54*, 513.
(66) Adachi, K.; Watari, H. *Chem.—Eur. J.* **2006**, *12*, 4249.
(67) Szejtli, J. *Chem. Rev.* **1998**, *98*, 1743.
(68) Correa, N. M.; Silber, J. J. *J. Mol. Liq.* **1997**, *72*, 163.

(69) Correa, N. M.; Durantini, J. J.; Silber, J. J. *J. Colloid Interface Sci*. **1998**, *208*, 96.

(70) Correa, N. M.; Durantini, J. J.; Silber, J. J. *J. Colloid Interface Sci*. **2001**, *240*, 573.

(71) Zingaretti, L.; Correa, N. M.; Boscatto, L.; Chiacchiera, S.; Durantini, E. N.; Bertolotti, S. G.; Rivarola, C. R.; Silber, J. J. *J. Colloid Interface Sci.* **2005**, *286*, 245.

(72) Sabadini, 0. E.; Cosgrove, T.; Egidio, F. C. *Carbohydr. Res.* **2006**, *341*, 270.

(73) Frankewich, R. P.; Thimmaiah, K. N.; Hinze, W. L. *Anal. Chem*. **1991**, *63*, 2924.

(74) Baruah, B.; Roden, J.; Sedgwick, M.; Correa, N. M.; Crans, D. C.; Levinger, N. E. *J. Am. Chem. Soc*. **2006**, *128*, 12758.

(75) Wu, J-S.; Toda, K.; Tanaka, A.; Sanemasa, I. *Bull. Chem. Soc. Jpn*. **1998**, *71*, 1615.

(76) Harada, A.; Hu, Y.; Yamamoto, S.; Takahashi, S. *J. Chem Soc., Dalton Trans*. **1988**, 729.

(77) Hwang, H. S.; Lee, M. Y.; Jeong, Y. T.; Hong, S.-S.; Gal, Y.-S.; Lim, K. T. *Ind. Eng. Chem. Res.* **2006**, *45*, 3434.

(78) It is very well-known that poly substitution of the OH of the cyclodextrin molecule leads to more water soluble compounds; see, for instance, Auzely-Velty, R.; Djedaïni-Pilard, F.; Desert, S.; Perly, B.; Zemb, T. *Langmuir* **2000**, *16*, 3727.

(79) This is the value reported from our laboratory. Barra, M.; de Rossi, R. H.; de Vargas, E. B. *J. Org. Chem* **1987**, *52*, 5004. Other reported values are even smaller; for instance, $K = 160\ M^{-1}$ is reported in the following: Wang, Y.; Eaton, D. F. *Chem. Phys. Lett.* **1985**, *120*, 441. It is also important to note that the association constants of β-CD and hp-β-CD are always very similar.

(80) (a) Zhong, Q.; Steinhurst, D. A.; Carpenter, E. E.; Owrutsky, J. C. *Langmuir* **2002**, *18*, 7401. (b) Faeder, J.; Landanyi, B. M. *J. Phys. Chem. B* **2001**, *105*, 11148. (c) Crans, D. C.; Rithner, C. D.; Baruah, B.; Gourley, B. L.; Levinger, N. E. *J. Am. Chem. Soc*. **2006**, *128*, 4437.

(81) Roberts, C. B.; Thompson, J. B. *J. Phys. Chem. B* **1998**, *102*, 9074.

(82) González-Blanco, C.; Rodríguez, L. J.; Velázquez, M. M. *J. Colloid Interface Sci*. **1999**, *211*, 380.

(83) Silber, J. J.; Falcone, R. D.; Correa, N. M.; Biasutti, M. A.; Abuin, E.; Lissi, E.; Campodonico, P. *Langmuir* **2003**, *19*, 2067.

(84) Shen, D.; Dong, Y.; Han, B.; Chen, J.; Zhang, J. *J. Colloid Interface Sci.* **2006**, *296*, 350.

(85) Shen, D.; Han, B.; Dong, Y.; Wu, W.; Chen, J.; Zhang, J. *Chem.—Eur. J*. **2005**, *11*, 1228.

(86) Liu, J.; Shervani, Z.; Raveendran, P.; Ikushima, Y. *J. Supercrit. Fluids* **2005**, *33*, 121.

(87) Liu, J.; Ikushima, Y.; Shervani, Z. *J. Supercrit. Fluids* **2004**, *32*, 97.

(88) Hutton, B. H.; Perera, J. M.; Grieser, F.; Stevens, G. W. *Colloids Surf., A* **1999**, *146*, 227.

(89) Gao, H.; Li, J.; Han, B.; Chen, W.; Zhang, J.; Zhang, R.; Yan, D. *Phys. Chem. Chem. Phys.* **2004**, *6*, 2914.

(90) Li, N.; Gao, Y.; Zheng, L.; Zhang, L.; Yu, L.; Li, X. *Langmuir* **2007**, *23*, 1091.

(91) Molina, P. G.; Silber, J. J.; Correa, N. M.; Sereno, L. *J. Phys. Chem. C* **2007**, *111*, 4269.

(92) Correa, N. M.; Biasutti, M. A.; Silber, J. J. *J. Colloid Interface Sci.* **1996**, *184*, 570.